



Enhanced Starting Track Real-time Stream for IceCube

Downloaded from: <https://research.chalmers.se>, 2025-06-01 07:51 UTC

Citation for the original published paper (version of record):

Mancina, S., Abbasi, R., Ackermann, M. et al (2024). Enhanced Starting Track Real-time Stream for IceCube. *Proceedings of Science*, 444

N.B. When citing this work, cite the original published paper.

Enhanced Starting Track Real-time Stream for IceCube

The IceCube Collaboration

(a complete list of authors can be found at the end of the proceedings)

E-mail: jsosborn2@wisc.edu

IceCube real-time alerts allow for rapid follow-up observations of likely astrophysical neutrino events, enabling searches for multi-messenger counterparts. The Enhanced Starting Track Real-time Stream (ESTReS) is a real-time extension of the Enhanced Starting Track Event Selection (ESTES), a high astrophysical purity muon-neutrino sample recently used by IceCube to measure the astrophysical diffuse flux. A set of computationally cheap cuts allows us to run a fast filter in seconds. This online filter selects about 100 events per day to be sent to Madison, WI via satellite where the full ESTES event selection is applied within minutes. Events that pass the final set of cuts (ESTReS + ESTES) will be sent out as real-time alerts to the broader astrophysical community. ESTReS's unique contribution to the current real-time alerts will be events in the southern sky in the 5 TeV - 100 TeV range. We expect about 10.3 events per year which average 50% astrophysical purity. In this talk I will report the status of the ESTReS alert stream in the context of the IceCube real-time program.

Corresponding authors: Jesse Osborn^{1*}, Sarah Mancina^{1,2}, Manuel Silva¹

¹ *University of Wisconsin, Madison*

² *Università Degli Studi di Padova*

* Presenter

The 38th International Cosmic Ray Conference (ICRC2023)
26 July – 3 August, 2023
Nagoya, Japan



1. Introduction

IceCube is a cubic-kilometer neutrino detector located at the South Pole [1] which completed construction in December 2010. It consists of digital-optical-modules (DOMs) containing photomultiplier tubes buried between 1450 m and 2450 m into the ice. It optically observes the Cherenkov radiation that is emitted by charged particles which are produced in the weak interactions between incoming neutrinos and the surrounding ice.

Since 2016 (and improved in 2019), IceCube has been sending out alerts for possible astrophysical neutrinos that are detected in real-time to the multi-messenger astrophysics community within minutes of detection. This real-time alert stream is made up of several different event selections which are detailed in Ref. [2]. We present a new event selection which will predominantly provide events from the southern sky and with reconstructed energies of 5-100 TeV. These events are currently not well covered by IceCube's real-time stream. We will be able to double the number of IceCube Gold (50% average astrophysical purity) alerts sent out per year, from ~ 10 to ~ 20 .

In Sec 2, we describe the new event selection for alerts, and the evaluated event rates using Monte Carlo (MC) and 10.3 years of archival data. In Sec 3, we describe the calculation of the signalness variable per event. In Sec 4, we detail the information that will be sent out as alerts to the community.

2. Event Selection

The dominant event morphology in this selection is starting tracks, generated predominantly by charged current muon neutrino interactions in the ice inside the detector's volume. Two examples are shown in Fig. 1. The zenith angle (θ) is in IceCube detector coordinates. $\theta = 0$ means coming from the southern sky, up towards the Earth, and $\theta = \pi$ means coming from the northern sky, down through the Earth.

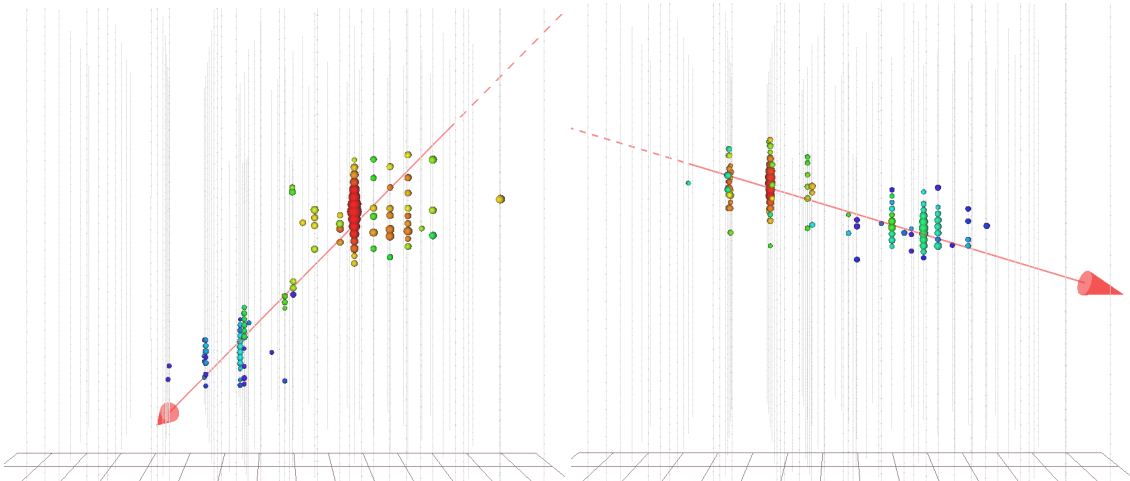


Figure 1: Display of two archival data events in the selection. (Left / Right): Reconstructed energy = 7.3 TeV / 9.8 TeV, reconstructed zenith = 53.6° / 73.5° , and signalness = 0.295 / 0.156 according to the sigmoid fit parameterization (see Eq. 2).

The event selection has two stages. The first is a series of computationally cheap cuts that are run in real-time on events at the South Pole to greatly reduce event rates. The second is a more computationally expensive set of cuts known as the Enhanced Starting Track Event Selection (ESTES), a high purity muon neutrino sample. Variations of ESTES with slightly different sets of cuts have been used for a neutrino source search [3] and for a measurement of the diffuse astrophysical flux [4–7].

2.1 At South Pole Selection

The following cuts are run at the South pole in sequential order to cut down event rates. These cuts make use of a directional reconstruction algorithm that is run at the South Pole, which is computationally cheap. Later on in the event selection, it is superseded by a more computationally intensive and effective directional reconstruction algorithm taken from ESTES (see the reconstructed cosine zenith in Figs. 2, 3, 4 and 5). The two algorithms do not always agree, especially for more poorly reconstructed events, where one algorithm may say it comes from the southern sky and the other may say it comes from the northern sky.

Each event must have:

1. At least 450 photoelectrons detected across all DOMs after the reconstructed interaction vertex time
2. Reconstructed zenith angle $\theta_{Pole} < 75^\circ$
 - (a) Different reconstruction algorithm from that shown in Figs. 2, 3, 4 and 5. Some events are miss-reconstructed at the South Pole (passing this $\theta_{Pole} < 75^\circ$ cut) and are later reconstructed by ESTES to be from the northern sky instead.
3. Probability of an event being an incoming muon < 0.001
 - (a) Derived from ESTES's Starting Track Veto, see §2.2
4. Length of the track inside the detector > 400 m

Events that pass all of these cuts will then be sent north and run through ESTES, which takes several minutes.

2.2 Enhanced Starting Track Event Selection

The ESTES event selection has been detailed in previous and concurrent ICRC contributions (see Ref. [3–6]). The key features are the Starting Track Veto, a cut which uses an event's reconstructed direction to define a dynamic veto region to heavily reduce atmospheric muon rates (see Fig. 1 in Ref. [5] and a Boosted Decision Tree classifier, which further reduces background rates. The remaining events form a high purity muon neutrino sample, dominated by southern sky neutrinos.

A measurement of the diffuse astrophysical neutrino flux using ESTES is detailed in a concurrent ICRC proceeding (see Ref. [6]). The Monte Carlo and data shown here are a direct subset of those shown in the ESTES diffuse analysis. This event selection makes use of the same variation of ESTES cuts used for the diffuse analysis. The addition of the cuts done at Pole make this subset have a far higher astrophysical neutrino purity than ESTES.

2.3 Expected Final Event Rates

To estimate the rate of astrophysical neutrino events, we use Monte Carlo and the results of the ESTES diffuse single power law fit (see Ref. [6]) for the astrophysical neutrinos, $\phi_{\text{Astro}}^{\text{per-flavor}} = 1.68$ and $\gamma_{\text{Astro}} = 2.58$ and their systematic uncertainties. To estimate the rate of atmospheric neutrino events, we used the GaisserH4a [8] cosmic ray model and the Sibyll2.3c [9] hadronic interaction model. Error bars on the expected rates are produced by sampling the parameters in the 68% error contour in $\phi_{\text{Astro}}^{\text{per-flavor}}$ vs γ_{Astro} space provided by the ESTES diffuse single power law fit [6, 7].

There are two variables of relevance: the reconstructed neutrino energy and the reconstructed cosine zenith, both of which are the same as used in the ESTES diffuse analysis. The reconstructed energy comes from the ESTES Random Forest algorithm (based off Ref. [10]). The reconstructed cosine zenith comes from the ESTES diffuse reconstruction algorithm using Millipede (see Ref. [6]).

The data/MC plots for these variables are shown in Fig. 2. The reconstructed energy shown here will also be sent out in the real-time alert. The reconstructed cosine zenith shown here will not be sent out in the real-time alert; a more robust method will be used instead (see §4).

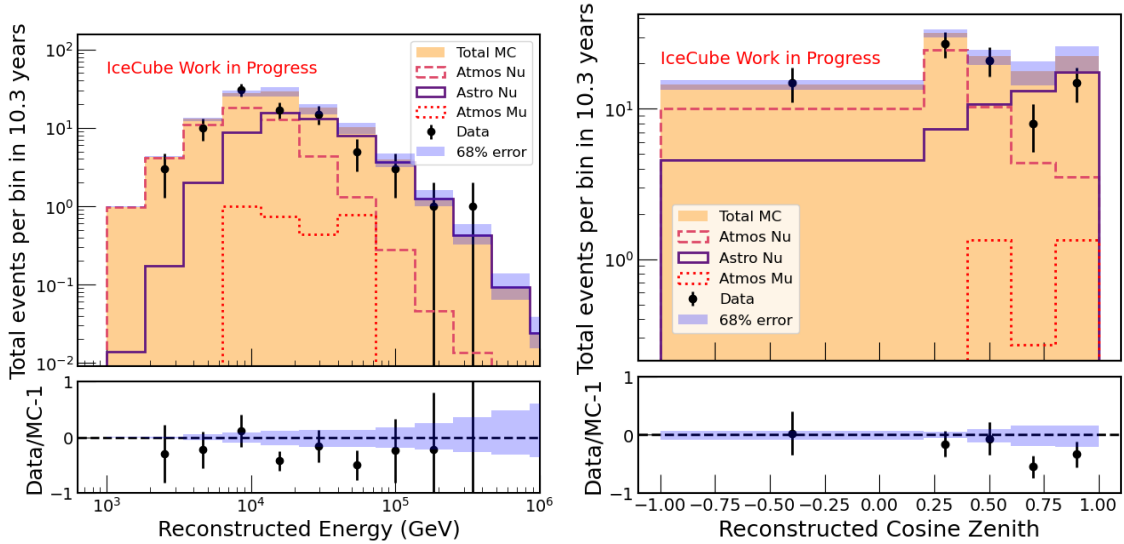


Figure 2: Data vs Monte Carlo comparisons for the energy and cosine zenith variables, which are used to define the signalness on a per event basis. The MC over predicts the data substantially in 2 energy bins and 1 cosine zenith bin, and work is in progress to resolve this.

There is currently an observed normalization issue where the MC over predicts the number of events compared to the data, which is most prominent in two energy bins and one cosine zenith bin in Fig. 2. The ESTES diffuse event selection observes good data/MC agreement in both of these parameters across the parameter space (see Fig. 3 in Ref. [6]), so this tension is derived solely from the cuts unique to the real-time process at Pole. Resolving this discrepancy is underway.

The reconstructed energy and cosine zenith are used to build our event rate expectations, as seen in Fig. 3. The Signal Alarm Rate (SAR) defines how many genuine astrophysical events will be sent out as alerts per year, and the False Alarm Rate (FAR) defines how many background events will be sent out as alerts per year.

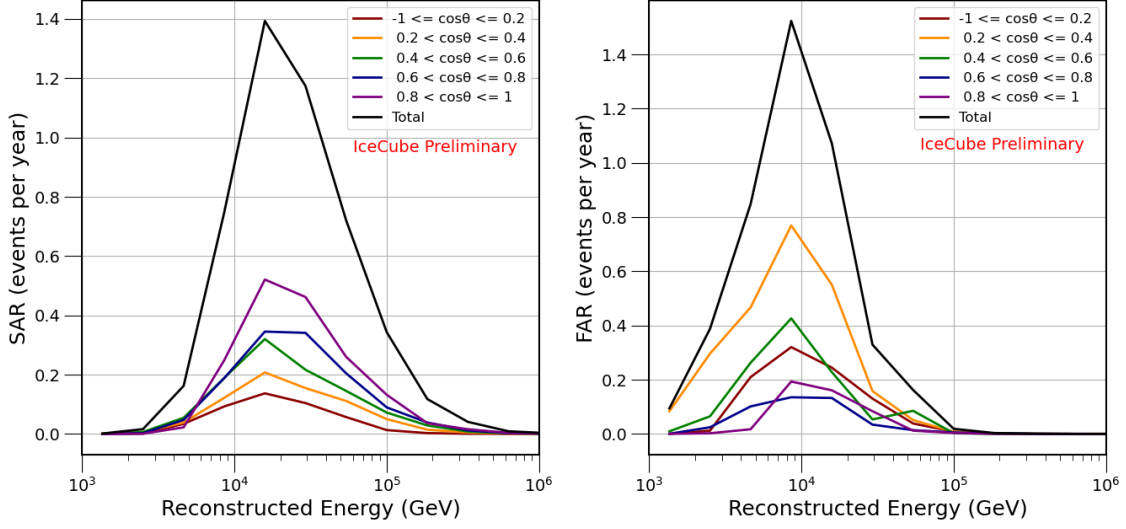


Figure 3: Left: Signal Alarm Rate vs energy, for each of the cosine zenith bins (total = 5.1 events per year). Right: False Alarm Rate vs energy for different cosine zenith bins (total = 5.2 events per year). The energy bin widths are the same as in Fig. 2.

In total, we expect 10.3 events per year to be sent out as alerts, 50% of which will be of astrophysical origin. This is the same purity standard as IceCube Gold real-time alerts, so this selection can be added directly into the current real-time stream. In looking at 10.3 years of archival data, there has been no observed overlap between this selection and any of IceCube's current real-time event selections (GFU, HESE and EHE in [2]).

3. Signalness Calculation

Because these events are sent out in real-time to other physics experiments, it is useful to quantify how interesting an event is with *signalness*, the probability that the event is astrophysical. We calculate the signalness on an event-by-event basis, first by taking our MC and splitting it into different energy and cosine zenith bins according to Fig. 2, which can be seen in Fig. 4. Formally,

$$\text{Signalness}(E, \theta) = \frac{N_{astro}(E, \theta)}{N_{astro}(E, \theta) + N_{bkg}(E, \theta)}, \quad (1)$$

where N_{astro} is the "Astro Nu" and N_{bkg} is the "Atmos Nu" and "Atmos Mu" as seen in Fig. 2 across the reconstructed energy and reconstructed cosine zenith space.

Then, we fit each reconstructed cosine zenith bin with a 1d sigmoid function in reconstructed energy space to interpolate $S(E, \theta)$ on an event by event basis. The sigmoid fit function for each reconstructed cosine zenith bin has 3 free parameters, and is given by

$$\text{Signalness} = \frac{1 - c}{1 + e^{-k_o(\log_{10}(E) + x_o)}} + c. \quad (2)$$

The sigmoid fits and their resultant signalness values can be seen in Fig. 5.

The final signalness distribution evaluated by Eq. 2 is shown in Fig. 6, and can be directly compared with the distribution of current alerts seen in Fig. 5 of Ref. [2]. This is calculated based

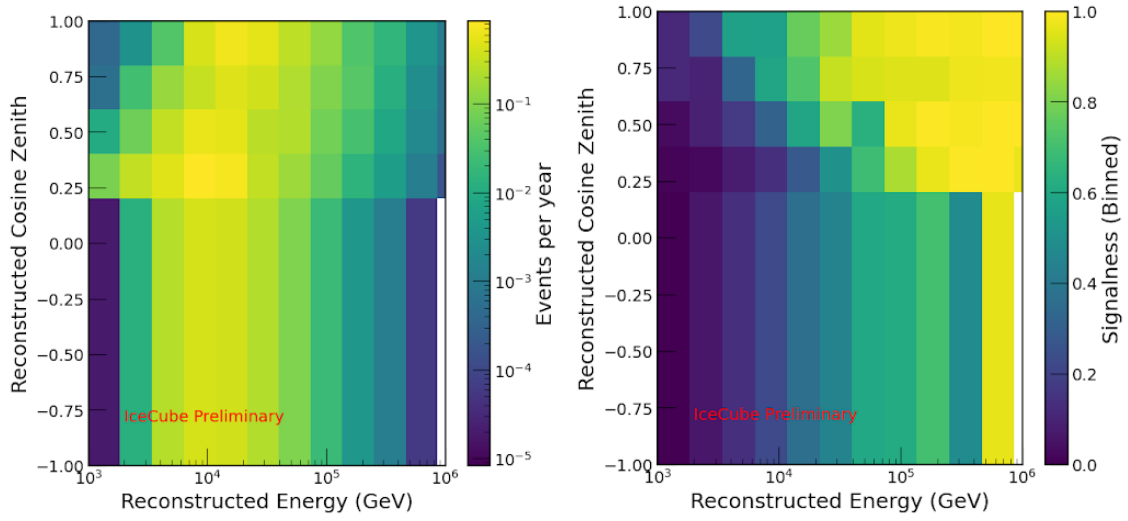


Figure 4: 2d histograms of the event rates (same as both panels of Fig. 3 added together) for this event selection (left) and the signalness of events in a given bin (right) binned in the reconstructed energy and reconstructed cosine zenith.

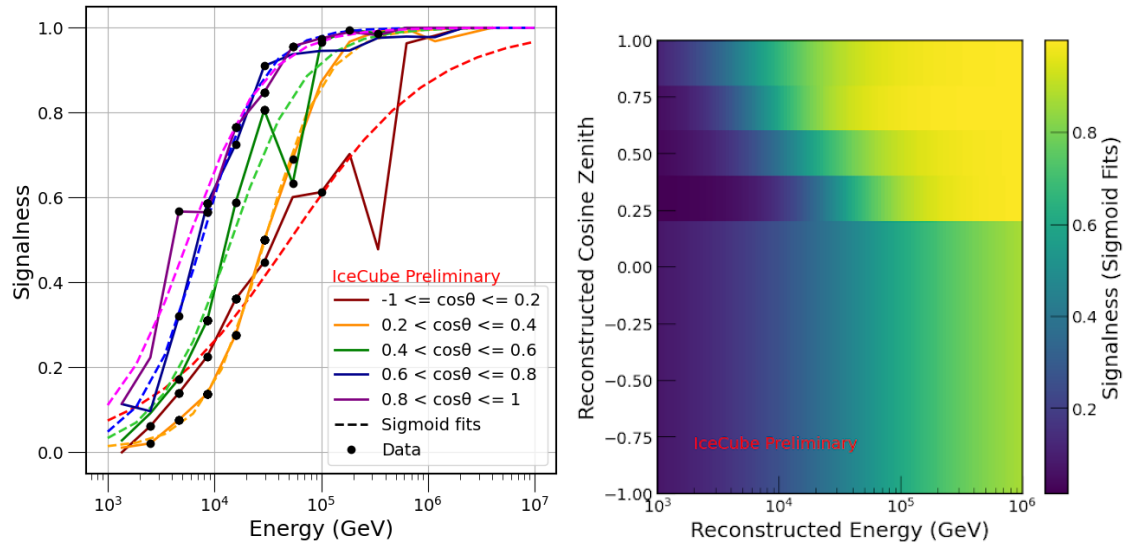


Figure 5: Left: 1d sigmoid fits to each of the cosine zenith bins shown in Fig. 4 across the energy range. Black data points represent cosine zenith/energy bins that contained archival data. Right: 2d histogram of the signalness of events according to the sigmoid fit parameterization.

off of the reconstructed energy and cosine zenith on a per event basis according to the sigmoid fit parameterization. This variable will be sent out in the real-time alert.

Here, we see that the events peak around a signalness of 0.2 and 0.8 and trough in the middle around 0.55.

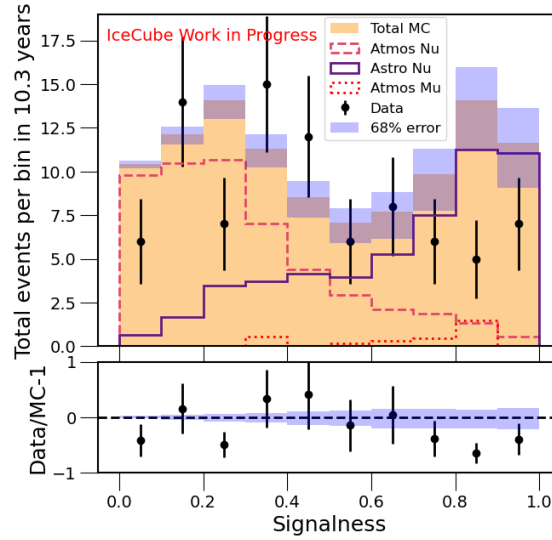


Figure 6: Data vs Monte Carlo comparison for the signalness evaluated by Eq. 2. The MC over predicts the data substantially in 3 signalness bins, a direct propagation of the data/MC mismatch seen in Fig. 2. Work is in progress to resolve this.

4. Real-time Alert Stream

All events that pass the event selection will be sent out as alerts in real-time, after running a final directional reconstruction algorithm, which performs a likelihood scan assuming the event originated from each pixel of the sky, iterating to more granular pixels as it approaches the best fit position (see Fig. 2 in Ref. [11]). The information sent to the multi-messenger community in the alert will be:

1. Timing information for the event
2. Reconstructed best fit direction in right ascension and declination evaluated by a likelihood scan of the entire sky
 - (a) Expect a median space angle resolution of 1.5° for alert events
3. Uncertainties on the right ascension and declination taken from the bounding rectangle on the 90% containment angular error contour, including a link to the likelihood skymap
 - (a) Expect median error in declination of $\pm 1.3^\circ$ and a median error in right ascension of $\pm 3^\circ$
4. Reconstructed energy of the event, taken from the ESTES Random Forest algorithm
 - (a) Energy resolution of 25% - 30% between 1 TeV and 10 PeV (see [6])
 - (b) Based off Ref. [10]
5. Signalness of the event, calculated as described above (sigmoid fits)

- (a) Expect an average event signalness of 50% (IceCube Gold)

There is currently ongoing work to refine the procedure for generating angular error contours for events sent out as alerts for this selection. This is due to observed under-coverage in our MC studies ($X\%$ containment contours cover the true event direction $< X\%$ of the time). This work may result in an additional cut on the event selection to remove events that are not well localized, or increased uncertainties on the right ascension and declination that get sent out as alerts.

5. Conclusion

Current estimates from the MC tell us that we expect 10.3 events per year from this alert stream. Given the fact that there has been no observed overlap at the alert level between this alert stream and the existing IceCube alert streams, these events would be unique additions to IceCube Gold, and would roughly double the number of IceCube Gold alerts sent out per year. These events would also open up more of the parameter space to the community, largely coming from the southern sky and at lower energies (mostly 5-100 TeV). This work is still undergoing development before being added to the IceCube real-time stream.

References

- [1] **IceCube** Collaboration, M. G. Aartsen *et al.* *JINST* **12** no. 03, (Mar, 2017) P03012.
- [2] **IceCube** Collaboration, R. Abbasi *et al.* (Apr, 2023) . arXiv:2304.01174.
- [3] **IceCube** Collaboration, S. Mancina and M. Silva *PoS ICRC2019* (2019) 954.
- [4] **IceCube** Collaboration, M. Silva and S. Mancina *PoS ICRC2019* (2019) 1010.
- [5] **IceCube** Collaboration, M. Silva and S. Mancina *PoS ICRC2021* (2021) 1130.
- [6] **IceCube** Collaboration, M. Silva *et al.* *PoS ICRC2023* (these proceedings) 1008.
- [7] **IceCube** Collaboration, M. G. Aartsen *et al.* *To be submitted to Physical Review D* .
- [8] T. K. Gaisser, T. Stanev, and S. Tilav *Frontiers of Physics* **8** (Apr, 2013) 748–758.
- [9] A. Fedynitch, F. Riehn, R. Engel, T. K. Gaisser, and T. Stanev *Phys. Rev. D* **100** (Nov, 2019) 103018.
- [10] **IceCube** Collaboration, M. G. Aartsen *et al.* *PoS Phys. Rev. D* (Nov, 2019) 99.
- [11] **IceCube** Collaboration, M. Lincetto *PoS ICRC2023* (these proceedings) 1106.

Full Author List: IceCube Collaboration

R. Abbasi¹⁷, M. Ackermann⁶³, J. Adams¹⁸, S. K. Agarwalla^{40, 64}, J. A. Aguilar¹², M. Ahlers²², J.M. Alameddine²³, N. M. Amin⁴⁴, K. Andeen⁴², G. Anton²⁶, C. Argüelles¹⁴, Y. Ashida⁵³, S. Athanasiadou⁶³, S. N. Axani⁴⁴, X. Bai⁵⁰, A. Balagopal V.⁴⁰, M. Baricevic⁴⁰, S. W. Barwick³⁰, V. Basu⁴⁰, R. Bay⁸, J. J. Beatty^{20, 21}, J. Becker Tjus^{11, 65}, J. Beise⁶¹, C. Bellenghi²⁷, C. Benning¹, S. BenZvi⁵², D. Berley¹⁹, E. Bernardini⁴⁸, D. Z. Besson³⁶, E. Blaufuss¹⁹, S. Blot⁶³, F. Bontempo³¹, J. Y. Book¹⁴, C. Boscolo Meneguolo⁴⁸, S. Böser⁴¹, O. Botner⁶¹, J. Böttcher⁴, E. Bourbeau²², J. Braun⁴⁰, B. Brinson⁶, J. Brostean-Kaiser⁶³, R. T. Burley², R. S. Busse⁴³, D. Butterfield⁴⁰, M. A. Campana⁴⁹, K. Carloni¹⁴, E. G. Carnie-Bronca², S. Chattopadhyay^{40, 64}, N. Chau¹², C. Chen⁶, Z. Chen⁵⁵, D. Chirkin⁴⁰, S. Choi⁵⁶, B. A. Clark¹⁹, L. Classen⁴³, A. Coleman⁶¹, G. H. Collin¹⁵, A. Connolly^{20, 21}, J. M. Conrad¹⁵, P. Coppin¹³, P. Correa¹³, D. F. Cowen^{59, 60}, P. Dave⁶, C. De Clercq¹³, J. J. DeLaunay⁵⁸, D. Delgado¹⁴, S. Deng¹, K. Deoskar⁵⁴, A. Desai⁴⁰, P. Desati⁴⁰, K. D. de Vries¹³, G. de Wasseige³⁷, T. DeYoung²⁴, A. Diaz¹⁵, J. C. Díaz-Vélez⁴⁰, M. Dittmer⁴³, A. Domi²⁶, H. Dujmovic⁴⁰, M. A. DuVernois⁴⁰, T. Ehrhardt⁴¹, P. Eller²⁷, E. Ellinger⁶², S. El Mentawi¹, D. Elsässer²³, R. Engel^{31, 32}, H. Erpenbeck⁴⁰, J. Evans¹⁹, P. A. Evenson⁴⁴, K. L. Fan¹⁹, K. Fang⁴⁰, K. Farrag¹⁶, A. R. Farrag¹⁶, A. Fedynitch⁵⁷, N. Feigl¹⁰, S. Fiedlschuster²⁶, C. Finley⁵⁴, L. Fischer⁶⁷, D. Fox⁵⁹, A. Frankowiak¹¹, A. Fritz⁴¹, P. Fürst¹, J. Gallagher³⁹, E. Ganster¹, A. Garcia¹⁴, L. Gerhardt⁹, A. Ghadimi⁵⁸, C. Glaser⁶¹, T. Glauch²⁷, T. Glüsenskamp^{26, 61}, N. Goehke³², J. G. Gonzalez⁴⁴, S. Goswami⁵⁸, D. Grant²⁴, S. J. Gray¹⁹, O. Gries¹, S. Griffin⁴⁰, S. Griswold⁵², K. M. Groth²², C. Günther¹, P. Gutjahr²³, C. Haack²⁶, A. Hallgren⁶¹, R. Halliday²⁴, L. Halve¹, F. Halzen⁴⁰, H. Hamdaoui⁵⁵, M. Ha Minh²⁷, K. Hanson⁴⁰, J. Hardin¹⁵, A. A. Harnisch²⁴, P. Hatch³³, A. Haungs³¹, K. Helbing⁶², J. Hellrung¹¹, F. Henningsen²⁷, L. Heuermann¹, N. Heyer⁶¹, S. Hickford⁶², A. Hidvegi⁵⁴, C. Hill¹⁶, G. C. Hill², K. D. Hoffman¹⁹, S. Hori⁴⁰, K. Hoshina^{40, 66}, W. Hou³¹, T. Huber³¹, K. Hultqvist²³, M. Hünnefeld²³, R. Hussain⁴⁰, K. Hymon²³, S. In⁵⁶, A. Ishihara¹⁶, M. Jacquart¹⁶, O. Janik¹, M. Jansson⁵⁴, G. S. Japaridze⁵, M. Jeong⁵⁶, M. Jin¹⁴, B. J. P. Jones⁴, D. Kang³¹, W. Kang⁵⁶, X. Kang⁴⁹, A. Kappes⁴³, D. Kappesser⁴¹, L. Kardum²³, T. Karg⁶³, M. Karle²⁷, A. Karle⁴⁰, U. Katz²⁶, M. Kauer⁴⁰, J. L. Kelley⁴⁰, A. Khatee Zathul⁴⁰, A. Kheirandish^{34, 35}, J. Kiryluk⁵⁵, S. R. Klein^{8, 9}, A. Kochocki²⁴, R. Koirala⁴⁴, H. Kolanoski¹⁰, T. Kontrimas²⁷, L. Köpke⁴¹, C. Kopper²⁶, D. J. Koskinen²², P. Koundal³¹, M. Kovacevich⁴⁹, M. Kowalski^{10, 63}, T. Kozynets²², J. Krishnamoorthi^{40, 64}, K. Kruijswijk³⁷, E. Krupczak²⁴, A. Kumar⁶³, E. Kun¹¹, N. Kurahashi⁴⁹, N. Lad⁶³, C. Lagunas Gualda⁶³, M. Lamoureux³⁷, M. J. Larson¹⁹, S. Latseva¹, F. Lauber⁶², J. P. Lazar^{14, 40}, J. W. Lee⁵⁶, K. Leonard DeHolton⁶⁰, A. Leszczyńska⁴⁴, M. Lincetto¹¹, Q. R. Liu⁴⁰, M. Liubarska²⁵, E. Lohfink⁴¹, C. Love⁴⁹, C. J. Lozano Mariscal⁴³, L. Lu⁴⁰, F. Lucarelli²⁸, W. Luszczyk^{20, 21}, Y. Lyu^{8, 9}, J. Madsen⁴⁰, K. B. M. Mahn²⁴, Y. Makino⁴⁰, E. Manao²⁷, S. Mancina^{40, 48}, W. Marie Sainte⁴⁰, I. C. Mariş¹², S. Marka⁴⁶, Z. Marka⁴⁶, M. Marsee⁵⁸, I. Martinez-Soler¹⁴, R. Maruyama⁴⁵, F. Mayhew²⁴, T. McElroy²⁵, F. McNally³⁸, J. V. Mead²², K. Meagher⁴⁰, S. Mechbal⁶³, A. Medina²¹, M. Meier¹⁶, Y. Merckx¹³, L. Merten¹¹, J. Micallef²⁴, J. Mitchell⁷, T. Montaruli²⁸, R. W. Moore²⁵, Y. Morii¹⁶, R. Morse⁴⁰, M. Moulai⁴⁰, T. Mukherjee³¹, R. Naab⁶³, R. Nagai¹⁶, M. Nakos⁴⁰, U. Naumann⁶², J. Necker⁶³, A. Negi⁴, M. Neumann⁴³, H. Niederhausen²⁴, M. U. Nisa²⁴, A. Noell¹, A. Novikov⁴⁴, S. C. Nowicki²⁴, A. Obertacke Pollmann¹⁶, V. O'Dell⁴⁰, M. Oehler³¹, B. Oeyen²⁹, A. Olivas¹⁹, R. Ørsøe²⁷, J. Osborn⁴⁰, E. O'Sullivan⁶¹, H. Pandya⁴⁴, N. Park³³, G. K. Parker⁴, E. N. Paudel⁴⁴, L. Paul^{42, 50}, C. Pérez de los Heros⁶¹, J. Peterson⁴⁰, S. Philippen¹, A. Pizzuto⁴⁰, M. Plum⁵⁰, A. Pontén⁶¹, Y. Popovych⁴¹, M. Prado Rodriguez⁴⁰, B. Pries²⁴, R. Procter-Murphy¹⁹, G. T. Przybylski⁹, C. Raab³⁷, J. Riedel⁴⁰, K. Rawlins³, Z. Rechac⁴⁰, A. Rehman⁴⁴, P. Reichherzer¹¹, G. Renzi¹², E. Resconi²⁷, S. Reusch⁶³, W. Rhode²³, B. Riedel⁴⁰, A. Rifaie¹, E. J. Roberts², S. Robertson^{8, 9}, S. Rodan⁵⁶, G. Roellinghoff⁵⁶, M. Rongen²⁶, C. Rott^{53, 56}, T. Ruhe²³, L. Ruohan²⁷, D. Ryckbosch²⁹, I. Safa^{14, 40}, J. Saffer³², D. Salazar-Gallegos²⁴, P. Sampathkumar³¹, S. E. Sanchez Herrera²⁴, A. Sandrock⁶², M. Santander⁵⁸, S. Sarkar²⁵, S. Sarkar⁴⁷, J. Savelberg¹, P. Savina⁴⁰, M. Schaufel¹, H. Schieler³¹, S. Schindler²⁶, L. Schlickmann¹, B. Schlüter⁴³, F. Schlüter¹², N. Schmeisser⁶², T. Schmidt¹⁹, J. Schneider²⁶, F. G. Schröder^{31, 44}, L. Schumacher²⁶, G. Schwefer¹, S. Sclafani¹⁹, D. Seckel⁴⁴, M. Seikh³⁶, S. Seunarine⁵¹, R. Shah⁴⁹, A. Sharma⁶¹, S. Shefali³², N. Shimizu¹⁶, M. Silva⁴⁰, B. Skrzypek¹⁴, B. Smithers⁴, R. Snihur⁴⁰, J. Soedingrekso²³, A. Sogaard²², D. Soldin³², P. Soldin¹, G. Sommani¹¹, C. Spannfellner²⁷, G. M. Spiczak⁵¹, C. Spiering⁶³, M. Stamatikos²¹, T. Stanev⁴⁴, T. Stetzelberger⁹, T. Stürwald⁶², T. Stuttard²², G. W. Sullivan¹⁹, I. Taboada⁶, S. Ter-Antonyan⁷, M. Thiesmeyer¹, W. G. Thompson¹⁴, J. Thwaites⁴⁰, S. Tilav⁴⁴, K. Tollefson²⁴, C. Tönnis⁵⁶, S. Toscano¹², D. Tosi⁴⁰, A. Trettin⁶³, C. F. Tung⁶, R. Turcotte³¹, J. P. Twagirayezu²⁴, B. Ty⁴⁰, M. A. Unland Elorrieta⁴³, A. K. Upadhyay^{40, 64}, K. Upshaw⁷, N. Valtonen-Mattila⁶¹, J. Vandenbroucke⁴⁰, N. van Eijndhoven¹³, D. Vannerom¹⁵, J. van Santen⁶³, J. Vara⁴³, J. Veitch-Michaelis⁴⁰, M. Venugopal³¹, M. Vereecken³⁷, S. Verpoest⁴⁴, D. Veske⁴⁶, A. Vijai¹⁹, C. Walck⁵⁴, C. Weaver²⁴, P. Weigel¹⁵, A. Weindl³¹, J. Weldert⁶⁰, C. Wendt⁴⁰, J. Werthebach²³, M. Weyrauch³¹, N. Whitehorn²⁴, C. H. Wiebusch¹, N. Willey²⁴, D. R. Williams⁵⁸, L. Witthaus²³, A. Wolf¹, M. Wolf²⁷, G. Wrede²⁶, X. W. Xu⁷, J. P. Yanez²⁵, E. Yildizci⁴⁰, S. Yoshida¹⁶, R. Young³⁶, F. Yu¹⁴, S. Yu²⁴, T. Yuan⁴⁰, Z. Zhang⁵⁵, P. Zhelnin¹⁴, M. Zimmerman⁴⁰

¹ III. Physikalisches Institut, RWTH Aachen University, D-52056 Aachen, Germany

² Department of Physics, University of Adelaide, Adelaide, 5005, Australia

³ Dept. of Physics and Astronomy, University of Alaska Anchorage, 3211 Providence Dr., Anchorage, AK 99508, USA

⁴ Dept. of Physics, University of Texas at Arlington, 502 Yates St., Science Hall Rm 108, Box 19059, Arlington, TX 76019, USA

⁵ CTSPS, Clark-Atlanta University, Atlanta, GA 30314, USA

⁶ School of Physics and Center for Relativistic Astrophysics, Georgia Institute of Technology, Atlanta, GA 30332, USA

⁷ Dept. of Physics, Southern University, Baton Rouge, LA 70813, USA

⁸ Dept. of Physics, University of California, Berkeley, CA 94720, USA

⁹ Lawrence Berkeley National Laboratory, Berkeley, CA 94720, USA

¹⁰ Institut für Physik, Humboldt-Universität zu Berlin, D-12489 Berlin, Germany

¹¹ Fakultät für Physik & Astronomie, Ruhr-Universität Bochum, D-44780 Bochum, Germany

¹² Université Libre de Bruxelles, Science Faculty CP230, B-1050 Brussels, Belgium

- ¹³ Vrije Universiteit Brussel (VUB), Dienst ELEM, B-1050 Brussels, Belgium
- ¹⁴ Department of Physics and Laboratory for Particle Physics and Cosmology, Harvard University, Cambridge, MA 02138, USA
- ¹⁵ Dept. of Physics, Massachusetts Institute of Technology, Cambridge, MA 02139, USA
- ¹⁶ Dept. of Physics and The International Center for Hadron Astrophysics, Chiba University, Chiba 263-8522, Japan
- ¹⁷ Department of Physics, Loyola University Chicago, Chicago, IL 60660, USA
- ¹⁸ Dept. of Physics and Astronomy, University of Canterbury, Private Bag 4800, Christchurch, New Zealand
- ¹⁹ Dept. of Physics, University of Maryland, College Park, MD 20742, USA
- ²⁰ Dept. of Astronomy, Ohio State University, Columbus, OH 43210, USA
- ²¹ Dept. of Physics and Center for Cosmology and Astro-Particle Physics, Ohio State University, Columbus, OH 43210, USA
- ²² Niels Bohr Institute, University of Copenhagen, DK-2100 Copenhagen, Denmark
- ²³ Dept. of Physics, TU Dortmund University, D-44221 Dortmund, Germany
- ²⁴ Dept. of Physics and Astronomy, Michigan State University, East Lansing, MI 48824, USA
- ²⁵ Dept. of Physics, University of Alberta, Edmonton, Alberta, Canada T6G 2E1
- ²⁶ Erlangen Centre for Astroparticle Physics, Friedrich-Alexander-Universität Erlangen-Nürnberg, D-91058 Erlangen, Germany
- ²⁷ Technical University of Munich, TUM School of Natural Sciences, Department of Physics, D-85748 Garching bei München, Germany
- ²⁸ Département de physique nucléaire et corpusculaire, Université de Genève, CH-1211 Genève, Switzerland
- ²⁹ Dept. of Physics and Astronomy, University of Gent, B-9000 Gent, Belgium
- ³⁰ Dept. of Physics and Astronomy, University of California, Irvine, CA 92697, USA
- ³¹ Karlsruhe Institute of Technology, Institute for Astroparticle Physics, D-76021 Karlsruhe, Germany
- ³² Karlsruhe Institute of Technology, Institute of Experimental Particle Physics, D-76021 Karlsruhe, Germany
- ³³ Dept. of Physics, Engineering Physics, and Astronomy, Queen's University, Kingston, ON K7L 3N6, Canada
- ³⁴ Department of Physics & Astronomy, University of Nevada, Las Vegas, NV, 89154, USA
- ³⁵ Nevada Center for Astrophysics, University of Nevada, Las Vegas, NV 89154, USA
- ³⁶ Dept. of Physics and Astronomy, University of Kansas, Lawrence, KS 66045, USA
- ³⁷ Centre for Cosmology, Particle Physics and Phenomenology - CP3, Université catholique de Louvain, Louvain-la-Neuve, Belgium
- ³⁸ Department of Physics, Mercer University, Macon, GA 31207-0001, USA
- ³⁹ Dept. of Astronomy, University of Wisconsin–Madison, Madison, WI 53706, USA
- ⁴⁰ Dept. of Physics and Wisconsin IceCube Particle Astrophysics Center, University of Wisconsin–Madison, Madison, WI 53706, USA
- ⁴¹ Institute of Physics, University of Mainz, Staudinger Weg 7, D-55099 Mainz, Germany
- ⁴² Department of Physics, Marquette University, Milwaukee, WI, 53201, USA
- ⁴³ Institut für Kernphysik, Westfälische Wilhelms-Universität Münster, D-48149 Münster, Germany
- ⁴⁴ Bartol Research Institute and Dept. of Physics and Astronomy, University of Delaware, Newark, DE 19716, USA
- ⁴⁵ Dept. of Physics, Yale University, New Haven, CT 06520, USA
- ⁴⁶ Columbia Astrophysics and Nevis Laboratories, Columbia University, New York, NY 10027, USA
- ⁴⁷ Dept. of Physics, University of Oxford, Parks Road, Oxford OX1 3PU, United Kingdom
- ⁴⁸ Dipartimento di Fisica e Astronomia Galileo Galilei, Università Degli Studi di Padova, 35122 Padova PD, Italy
- ⁴⁹ Dept. of Physics, Drexel University, 3141 Chestnut Street, Philadelphia, PA 19104, USA
- ⁵⁰ Physics Department, South Dakota School of Mines and Technology, Rapid City, SD 57701, USA
- ⁵¹ Dept. of Physics, University of Wisconsin, River Falls, WI 54022, USA
- ⁵² Dept. of Physics and Astronomy, University of Rochester, Rochester, NY 14627, USA
- ⁵³ Department of Physics and Astronomy, University of Utah, Salt Lake City, UT 84112, USA
- ⁵⁴ Oskar Klein Centre and Dept. of Physics, Stockholm University, SE-10691 Stockholm, Sweden
- ⁵⁵ Dept. of Physics and Astronomy, Stony Brook University, Stony Brook, NY 11794-3800, USA
- ⁵⁶ Dept. of Physics, Sungkyunkwan University, Suwon 16419, Korea
- ⁵⁷ Institute of Physics, Academia Sinica, Taipei, 11529, Taiwan
- ⁵⁸ Dept. of Physics and Astronomy, University of Alabama, Tuscaloosa, AL 35487, USA
- ⁵⁹ Dept. of Astronomy and Astrophysics, Pennsylvania State University, University Park, PA 16802, USA
- ⁶⁰ Dept. of Physics, Pennsylvania State University, University Park, PA 16802, USA
- ⁶¹ Dept. of Physics and Astronomy, Uppsala University, Box 516, S-75120 Uppsala, Sweden
- ⁶² Dept. of Physics, University of Wuppertal, D-42119 Wuppertal, Germany
- ⁶³ Deutsches Elektronen-Synchrotron DESY, Platanenallee 6, 15738 Zeuthen, Germany
- ⁶⁴ Institute of Physics, Sachivalaya Marg, Sainik School Post, Bhubaneswar 751005, India
- ⁶⁵ Department of Space, Earth and Environment, Chalmers University of Technology, 412 96 Gothenburg, Sweden
- ⁶⁶ Earthquake Research Institute, University of Tokyo, Bunkyo, Tokyo 113-0032, Japan

Acknowledgements

The authors gratefully acknowledge the support from the following agencies and institutions: USA – U.S. National Science Foundation-Office of Polar Programs, U.S. National Science Foundation-Physics Division, U.S. National Science Foundation-EPSCoR, Wisconsin Alumni Research Foundation, Center for High Throughput Computing (CHTC) at the University of Wisconsin–Madison, Open Science

Grid (OSG), Advanced Cyberinfrastructure Coordination Ecosystem: Services & Support (ACCESS), Frontera computing project at the Texas Advanced Computing Center, U.S. Department of Energy-National Energy Research Scientific Computing Center, Particle astrophysics research computing center at the University of Maryland, Institute for Cyber-Enabled Research at Michigan State University, and Astroparticle physics computational facility at Marquette University; Belgium – Funds for Scientific Research (FRS-FNRS and FWO), FWO Odysseus and Big Science programmes, and Belgian Federal Science Policy Office (Belspo); Germany – Bundesministerium für Bildung und Forschung (BMBF), Deutsche Forschungsgemeinschaft (DFG), Helmholtz Alliance for Astroparticle Physics (HAP), Initiative and Networking Fund of the Helmholtz Association, Deutsches Elektronen Synchrotron (DESY), and High Performance Computing cluster of the RWTH Aachen; Sweden – Swedish Research Council, Swedish Polar Research Secretariat, Swedish National Infrastructure for Computing (SNIC), and Knut and Alice Wallenberg Foundation; European Union – EGI Advanced Computing for research; Australia – Australian Research Council; Canada – Natural Sciences and Engineering Research Council of Canada, Calcul Québec, Compute Ontario, Canada Foundation for Innovation, WestGrid, and Compute Canada; Denmark – Villum Fonden, Carlsberg Foundation, and European Commission; New Zealand – Marsden Fund; Japan – Japan Society for Promotion of Science (JSPS) and Institute for Global Prominent Research (IGPR) of Chiba University; Korea – National Research Foundation of Korea (NRF); Switzerland – Swiss National Science Foundation (SNSF); United Kingdom – Department of Physics, University of Oxford.